Finite-Time Boundedness of Impulsive Delayed Reaction–Diffusion Stochastic Neural Networks

Yao, Qi; Wei, Tengda; Lin, Ping; Wang, Linshan

Published in:
IEEE Transactions on Neural Networks and Learning Systems

DOI:
10.1109/TNNLS.2024.3360711

Publication date:
2024

Finite-time boundedness of impulsive delayed reaction-diffusion stochastic neural networks

Qi Yao, Tengda Wei, Ping Lin, and Linshan Wang, *Member, IEEE,*

***Abstract*—Considering the impulsive delayed reaction-diffusion stochastic neural networks (IDRDSNNs) with hybrid impulses, the finite-time boundedness (FTB) and finite-time contractive boundedness (FTCB) are investigated in this paper. First, a novel delay integral inequality is presented. By integrating this inequality with the comparison principle, some sufficient conditions that ensure the FTB and FTCB of IDRDSNNs are obtained. This study demonstrates that the FTB of neural networks with hybrid impulses can be maintained, even in the presence of impulsive perturbations. And for a system that is not FTB due to impulsive perturbations, achieving FTB is possible through the implementation of appropriate impulsive control and optimization of the average impulsive intervals. In addition, to validate the practicality of our results, three illustrative examples are provided. In the end, these theoretical findings are successfully applied to image encryption.**

***Index Terms*—Finite-time boundedness, finite-time contractive boundedness, reaction-diffusion stochastic neural networks, impulses, delays**

I. Introduction

FINITE-TIME boundedness (FTB) is a concept distinct from the traditional Lyapunov asymptotic stability (LAS). Lyapunov asymptotic stability evaluates the system's behavior as time towards infinity, which is crucial for systems designed to operate indefinitely. However, FTB focuses on the state bounds within specific finite-time intervals. This distinction has real-world implications. Systems like aircraft controls, neural networks, and others, often operate within defined temporal parameters, so ensuring boundedness of states within finite-time frames is imperative. For instance, failing to ensure that an aircraft's control state remains within specific bounds over a defined period could have dire consequences. Similarly, in neural networks, without FTB, there could be significant deviations leading to erroneous outcomes. Hence, many researchers have explored state bounds within finite-time intervals [1–4].

The authors would like to thank the editor and reviewers for their insightful and constructive comments. This work was supported in part by the National Natural Science Foundation of China under Grant 32072976 and 62203284, in part by the Natural Science Foundation of Shandong Province under Grant ZR2022QA037, in part by the Fundamental Research Funds for the Central Universities under Grant 21CX06043A. (*Corresponding authors: Ping Lin; Linshan Wang.*)

Qi Yao is with the College of Science, China University of Petroleum (East China), Qingdao, 266580 China (email: yaoqi@upc.edu.cn).

Tengda Wei is with the School of Mathematics and Statistics, Shandong Normal University, Ji'nan, 250014 China (email: tdwei123@sdnu.edu.cn)

Ping Lin is with the Department of Mathematics, University of Dundee, Dundee, DD1 4HN U.K. (email: plin@maths.dundee.ac.uk).

Linshan Wang is with the School of Mathematical Sciences, Ocean University of China, Qingdao, 266100 China (email: wangls@ouc.edu.cn)

Recently, the FTB of various systems has garnered significant research interest [5–8]. For example, Amato et al. [6] studied the FTB of impulsive linear dynamical systems, deriving the necessary and sufficient conditions based on the solution of a coupled differential difference Lyapunov equation. Li et al. [7] introduced the Lyapunov-Razumikhin approach for the FTB of delayed systems and, using this method, derived sufficient conditions for the FTB of linear time-varying delayed systems. And [8] investigated the FTB of delayed fractional-order fuzzy cellular neural networks in terms of a new fractional-order Gronwall inequality with time delay.

However, practical applications often present additional complexity. For high-stakes systems such as chemical plants and transportation systems, merely requiring state bounds within finite-time intervals is insufficient. These systems, due to their intrinsic complexities and high operational risks, demand not just boundedness, but also considerations for state contraction and other stringent conditions [9]. Recognizing this requirement, researchers introduced the concept of finite-time contractive boundedness (FTCB) [10]. Finite-time contractive boundedness requires that the FTB states reside within a more restrictive bound compared to the initial data's bound prior to the final time. Since then, numerous studies have investigated both FTB and FTCB in various systems [7, 11, 12].

The delayed reaction-diffusion stochastic neural networks (DRDSNNs) stand as a system of particular interest, highlighting the intricacies and potentialities of FTB and FTCB research [13–15]. These networks, which consider time delays, diffusion effects, and stochastic disturbances, reflect network models prevalent in real-world scenarios. Integrating time delays into the networks can lead to state instabilities and oscillations, and can also diminish the inherent Markovian nature of the networks [16]. Concurrently, while the introduction of diffusions can modulate response speeds, it also broadens the spatial dimensionality, further complicating the research problem [17]. Additionally, stochastic perturbations present challenges by necessitating the use of both deterministic Lebesgue integration and uncertain Itô integration, and have the potential to shift system states [18].

Moreover, impulses are a critical feature in various systems, exerting significant influence on system behavior [19]. While research typically categorizes these as either stabilizing or destabilizing impulses, both types coexist in practical scenarios, such as neural networks, adding an element of unpredictability [17, 20–24]. To address this, our work integrates both kinds of impulses for a more comprehensive study. This dual-impulse approach provides several advantages, particu-

larly in the context of neural networks. Stabilizing impulses contribute to system stability and functionality, whereas destabilizing impulses introduce necessary plasticity, allowing the system to adapt to changing conditions and escape harmful local minima [25].

In addition, the studies by Chen et al. [26] have considered impulsive delayed reaction-diffusion neural networks, highlighting their practicality in image encryption applications. Similarly, Ganesan et al. [27] have examined neural networks with stochastic perturbations and time delays, further extending their results to image encryption as well. These studies collectively underscore the practical viability of such neural network models. Therefore, the neural network model, which combines time delays, diffusions, stochastic perturbations, and both kinds of impulses, offers a more realistic representation of real-world systems, enhances robustness, and allows for performance optimization.[28] Hitherto, there have been few findings reported concerning the FTB and FTCB of impulsive DRDSNNs (IDRDSNNs) with these two types of impulses.

Thus, this paper conducts an investigation into the FTB and FTCB of IDRDSNNs with hybrid impulses. The main contributions are summarized as follows: (1) A novel delay integral inequality is derived for two cases. This inequality generalizes the differential inequality in Theorem 3.1 in [29], Lemma 5 in [30] and Theorem 1.3.1 in [31], and it effectively handles the intrinsic characteristics of the time delays in our systems. The tailored inequality is crucial for studying the FTB and FTCB of IDRDSNNs. (2) The investigation encompasses both stabilizing and destabilizing impulses. Notably, we eliminate the common threshold associated with hybrid impulses, a limitation often encountered in existing research results, such as [32–34]. (3) Several sufficient conditions for the FTB, FTCB, and exponential stability of IDRDSNNs are presented by the obtained inequality and comparison principle. This analysis reveals that the FTB of neural networks with hybrid impulses can be effectively retained, even in the presence of impulsive perturbations. Additionally, in cases where the FTB of networks is disrupted by impulsive perturbations, it can be reestablished through careful regulation of impulsive controls and the optimization of average impulsive intervals.

The subsequent sections of the paper are structured hereafter: Section II introduces the IDRDSNNs and covers preliminaries. Section III presents a new delay integral inequality, and studies FTB, FTCB and exponential stability of IDRDSNNs via the presented inequality and comparison principle. Section IV consists of a series of numerical simulations demonstrating the efficacy of obtained results. And the final section summarizes the paper and provides a discussion of the results.

II. Preliminaries

Notations: Let $\mathbb{R}^l$ denote the l-dimensional real space accompanied by the Euclidean norm $|\cdot|$, $\mathbb{Z}_+$ represent the positive integer set, and $\boldsymbol{I}$ symbolize the identity matrix. The probability space $(\Omega, \mathscr{F}, \mathbb{P})$ is complete, with filtration $\{\mathscr{F}_t\}_{t\geq 0}$. The Hilbert space $L^2(\mathcal{O})^n$ is a vector space with the inner product $(\boldsymbol{u}, \boldsymbol{v}) = \int_{\mathcal{O}} \boldsymbol{u}(t,\boldsymbol{x})\boldsymbol{v}(t,\boldsymbol{x})\mathrm{d}\boldsymbol{x}$, and the norm $\|\boldsymbol{u}\| = \sqrt{(\boldsymbol{u},\boldsymbol{u})}$. Meanwhile, the norm of the Hilbert space $H_0^1(\mathcal{O})$ is given by $|||\boldsymbol{u}||| = ||\nabla \boldsymbol{u}||$. $H^2(\mathcal{O})^n$ represents the space of vector-valued functions defined on $\mathcal{O}$, which have square-integrable derivatives up to the second order. The Banach space PC_τ^b consists of all functions $\boldsymbol{\phi} : [-\tau, 0] \times \mathcal{O} \to L^2(\mathcal{O})^n$ that are piecewise left continuous, with their norm $\|\boldsymbol{\phi}\|_C$ defined as $\sup_{\theta\in[-\tau,0]} \|\boldsymbol{\phi}(\theta,\boldsymbol{x})\|$. Let $PC^b_{\mathscr{F}_0}$ represent the family of PC_τ^b-valued stochastic variables $\boldsymbol{\phi}$ that are $\mathscr{F}_0$-measurable and satisfy $E||\boldsymbol{\phi}||_C < \infty$. The left sided limit of $\boldsymbol{u}(t_k)$ is denoted by $\boldsymbol{u}(t_k^-)$, and the limit from the right is represented by $\boldsymbol{u}(t_k^+)$. Regarding the definition of the lower left Dini derivative for $\varphi(t)$, it is given by $D_-\varphi(t) \triangleq \liminf_{\triangle t\to 0^-} \frac{\varphi(t+\triangle t)-\varphi(t)}{\triangle t}$. The Frobenius norm denoted as $||\boldsymbol{B}||_F$, is calculated as $\sqrt{\mathrm{tr}(\boldsymbol{B}\boldsymbol{B}^T)}$, with $\boldsymbol{B}$ being an $n \times m$ matrix, and tr representing the trace operator. The set $M_2^{n,m}[0,t]$ comprises all the nonanticipating functions $G(t,\omega)$ that yield $n \times m$ matrix-valued outputs and almost surely satisfy $\int_0^t |G(s,\omega)|^2\mathrm{d}s < \infty$. Moreover, $M_2^{n,m} = \bigcap_{t>0} M_2^{n,m}[0,t]$. Lastly, the space $\mathscr{L}_2^0(Q^{\frac{1}{2}}(L^2(\mathcal{O})^m), L^2(\mathcal{O})^n)$ contains all Hilbert-Schmidt operators $\Phi : Q^{\frac{1}{2}}(L^2(\mathcal{O})^m) \to L^2(\mathcal{O})^n$, accompanied by the norm $||\Phi||_* = \sqrt{\mathrm{tr}(\Phi Q \Phi^*)}$, where Q is a Hilbert-Schmidt operator with a finite trace, which is positive definite and self-adjoint, and Φ^* denotes the adjoint of Φ.

In this paper, we consider the IDRDSNNs as follows.

$$\begin{cases} \mathrm{d}\boldsymbol{u} = (\mathscr{A}\boldsymbol{u} - \boldsymbol{A}\boldsymbol{u} + \boldsymbol{B}\boldsymbol{f}(\boldsymbol{u}) + \boldsymbol{C}\boldsymbol{h}(\boldsymbol{u}(t-\tau,\boldsymbol{x})))\mathrm{d}t \\ \qquad\quad +\boldsymbol{G}(\boldsymbol{u}(t-\tau,\boldsymbol{x}))\mathrm{d}\boldsymbol{W}(t,\boldsymbol{x}),\ t \in (t_{k-1}, t_k), \\ \boldsymbol{u}(t_k^+,\boldsymbol{x}) = \delta_k \boldsymbol{u}(t_k,\boldsymbol{x}),\ k \in \mathbb{Z}_+, \\ \boldsymbol{u}(t,\boldsymbol{x})\,|_{\boldsymbol{x}\in\partial\mathcal{O}} = 0,\ t \geq 0, \\ \boldsymbol{u}(\theta,\boldsymbol{x},\omega) = \boldsymbol{\phi}(\theta,\boldsymbol{x},\omega) \in PC^b_{\mathscr{F}_0}, \end{cases} \tag{1}$$

where $\theta \in [-\tau, 0]$, $\boldsymbol{x} \in \mathcal{O}$, $\omega \in \Omega$, and $\boldsymbol{u} = (u_1(t,\boldsymbol{x},\omega), u_2(t,\boldsymbol{x},\omega), \cdots, u_n(t,\boldsymbol{x},\omega))^T$. The linear operator $\mathscr{A}$, defined as $\mathscr{A}\boldsymbol{u} = (\sum_{j=1}^l \frac{\partial(D_{1j}(\boldsymbol{x})\frac{\partial u_1}{\partial x_j})}{\partial x_j}, \sum_{j=1}^l \frac{\partial(D_{2j}(\boldsymbol{x})\frac{\partial u_2}{\partial x_j})}{\partial x_j}, \cdots, \sum_{j=1}^l \frac{\partial(D_{nj}(\boldsymbol{x})\frac{\partial u_n}{\partial x_j})}{\partial x_j})^T$, has its domain $\mathcal{D}(\mathscr{A})$ as the intersection of $H_0^1(\mathcal{O})^n$ and $H^2(\mathcal{O})^n$, which is a subset of $L^2(\mathcal{O})^n$. $\boldsymbol{A}$ is an n-dimensional diagonal matrix with all elements greater than zero, while $\boldsymbol{B}$ and $\boldsymbol{C}$ are both $n \times n$ matrices. $\boldsymbol{f}(\boldsymbol{u}) = (f_1(u_1), f_2(u_2), \cdots, f_n(u_n))^T$, $\boldsymbol{h}(\boldsymbol{u}(t-\tau,\boldsymbol{x})) = (h_1(u_1(t-\tau,\boldsymbol{x})), h_2(u_2(t-\tau,\boldsymbol{x})), \cdots, h_n(u_n(t-\tau,\boldsymbol{x})))^T$, $\boldsymbol{G} = (G_{ij})_{n\times m} \in M_2^{n,m}$, and $\boldsymbol{W}(t,\boldsymbol{x})$ denotes an m-dimensional Q-Wiener process [35]. The strength of impulses is represented by $\delta_k \in \mathbb{R}$. To avoid accumulation points, we assume that impulse time sequences satisfy $0 = t_0 < t_1 < \cdots < t_{N(0,T)} \leq T$, denoted by set $\mathcal{F}_0$. For any given positive constant η, $\mathcal{F}(\eta)$ represents the collection of impulse time sequences from $\mathcal{F}_0$ that satisfy $t_k - t_{k-1} \geq \eta$ for all $k \in \mathbb{Z}_+$. In addition, the initial data is represented by $\boldsymbol{\phi}(\theta,\boldsymbol{x},\omega)$, and $\mathcal{O} \subset \mathbb{R}^l$ is a bounded, open, and connected set featuring a sufficiently smooth boundary $\partial\mathcal{O}$.

Without loss of generality, we assume that the strengths of the destabilizing and stabilizing impulses are selected from $\overline{\Delta} = \{\overline{\delta_1}, \overline{\delta_2}, \cdots, \overline{\delta_N}\}$ and $\underline{\Delta} = \{\underline{\delta_1}, \underline{\delta_2}, \cdots, \underline{\delta_M}\}$, respectively, over the interval $(0, T]$. For these selections, we ensure that $|\overline{\delta_i}| > 1$ for $i = 1, 2, \cdots, N$, and $0 < |\underline{\delta_j}| < 1$ for $j = 1, 2, \cdots, M$. We use $t_{ik\uparrow}$ and $t_{jk\downarrow}$ which belong

to the set $\{t_1, t_2, \cdots, t_{N(0,T)}\}$, to denote the activation time of $\overline{\delta_i}$ and $\underline{\delta_j}$, respectively. Furthermore, we suppose that $\boldsymbol{f}(\boldsymbol{0}) = \boldsymbol{h}(\boldsymbol{0}) = \boldsymbol{0}$, and $\boldsymbol{G}(\boldsymbol{0}) = \boldsymbol{0}$.

For (1), we assume the subsequent conditions:

(A_1) There exists a constant $\alpha > 0$ ensuring $D_{ij}(\boldsymbol{x}) \geq \alpha$, for $i = 1, 2, \cdots, n$ and $j = 1, 2, \cdots, l$.

(A_2) The functions $\boldsymbol{f}(\boldsymbol{u})$, $\boldsymbol{h}(\boldsymbol{u})$, and $\boldsymbol{G}(\boldsymbol{u})$ all satisfy the Lipschitz condition, that is, a nonnegative constant ρ exists such that the following inequality holds: $\sup\{||\boldsymbol{f}(\boldsymbol{u}) - \boldsymbol{f}(\boldsymbol{v})||, ||\boldsymbol{h}(\boldsymbol{u}) - \boldsymbol{h}(\boldsymbol{v})||, ||\boldsymbol{G}(\boldsymbol{u}) - \boldsymbol{G}(\boldsymbol{v})||_*\} \leq \rho||\boldsymbol{u} - \boldsymbol{v}||$.

Based on Theorem 3.2 in [36] and Theorem 1 in [37], we can establish the existence and uniqueness of the solution to (1).

Definition 1 ([38]). *For impulsive sequences $\{t_{ik\uparrow}\}$ and $\{t_{jk\downarrow}\}$, the average impulsive intervals, denoted by T_{iA} and T_{ja} respectively, are defined under the condition:*

$$\overline{N_i}(t,s) \leq \frac{t-s}{T_{iA}} + N_0, \quad \underline{N_j}(t,s) \geq \frac{t-s}{T_{ja}} - N_0, \tag{2}$$

where N_0 is an positive integer, and $\overline{N_i}(t,s)$ and $\underline{N_j}(t,s)$ count the impulsive times in their sequences over (s,t).

Definition 2 ([6]). *Provided with three positive numbers T, κ_1, and κ_2 such that $\kappa_2 > \kappa_1$, then (1) is FTB concerning (T, κ_1, κ_2), if satisfying $E||\boldsymbol{\phi}(\theta)||_C^2 \leq \kappa_1$ results in $E||\boldsymbol{u}(t)||^2 \leq \kappa_2$ for any $t \in [0,T]$.*

Definition 3 ([6]). *Provided with five positive numbers T, κ_1, κ_2, κ_3, and σ such that $\kappa_2 > \kappa_1 > \kappa_3$, and $\sigma \in (0,T)$, (1) is defined as FTCS with respect to $(T, \kappa_1, \kappa_2, \kappa_3, \sigma)$, if $E||\boldsymbol{\phi}(\theta)||_C^2 \leq \kappa_1$ leads to $E||\boldsymbol{u}(t)||^2 \leq \kappa_2$ for any $t \in [0,T]$, and in addition, $E||\boldsymbol{u}(t)||^2 \leq \kappa_3$ for any $t \in [T-\sigma, T]$.*

Lemma 1 (Comparison Principle [39]). *$\mu(t)$ and $\nu(t)$ are supposed to be elements of $PC([-\tau, T], \mathbb{R})$ and adhere to the subsequent inequalities:*

$$\begin{cases} D_-\mu(t) > \Gamma(t, \mu(t), \overline{\mu}(t)), \ t \in (t_{k-1}, t_k), \\ \mu(t_k^+) \geq I_k(\mu(t_k)), \ k \in \mathbb{Z}_+, \end{cases} \tag{3}$$

$$\begin{cases} D_-\nu(t) \leq \Gamma(t, \nu(t), \overline{\nu}(t)), \ t \in (t_{k-1}, t_k), \\ \nu(t_k^+) \leq I_k(\nu(t_k)), \ k \in \mathbb{Z}_+, \end{cases} \tag{4}$$

where the functions $\overline{\mu}(t) = \sup_{\theta \in [-\tau, 0]} \mu(t+\theta)$, and $\overline{\nu}(t) = \sup_{\theta \in [-\tau, 0]} \nu(t+\theta)$. $\Gamma(t, x, y)$ is continuous and is nondecreasing concerning y when (t, x) is fixed. Additionally, $I_k(x)$ is nondecreasing regarding x for $k \in \mathbb{Z}_+$. If $\mu(t) \geq \nu(t)$ over the interval $[-\tau, 0]$, it follows that $\mu(t) \geq \nu(t)$ over the interval $[0, T]$.

III. Main Results

In the section herein, we obtain several sufficient conditions ensuring the FTB and FTCB of (1). Additionally, our analysis also contributes to the derivation of exponential stability.

Lemma 2. *Consider $v(t) \geq 0$, which fulfills the inequalities:*

$$\begin{cases} v(t) \leq k_1\overline{v}(0)e^{k_2 t} + \int_0^t e^{k_2(t-s)}[k_3 v(s-\tau) \\ \qquad +k_4]\mathrm{d}s, \quad t \in (0,T], \\ v(\theta) \geq 0, \quad t \in [-\tau, 0], \end{cases} \tag{5}$$

where $k_1 > 1$, $k_3 > 0$, $k_4 > 0$, and $\overline{v}(0) = \sup_{\theta \in [-\tau, 0]} v(\theta)$.

(1) If $k_2 < -k_3 < 0$, then $v(t) \leq k_1\overline{v}(0)e^{\lambda t} + \frac{k_4}{-k_2-k_3}$, where $\lambda < 0$ satisfies that $\lambda - k_2 = k_3 e^{-\lambda\tau}$;

(2) If $-k_3 e^{-k_2\tau} \leq k_2$, then $v(t) \leq [(k_1 + k_3\tau e^{-k_2\tau})\overline{v}(0) + k_4\int_0^t e^{-k_2 s}\mathrm{d}s]e^{(k_3 e^{-k_2\tau}+k_2)t}$.

Proof: (1) If $k_2 < -k_3 < 0$, then we define $h(\upsilon) = -\upsilon + k_3 e^{-\upsilon\tau} + k_2$. It follows that $h(0) = k_3 + k_2 < 0$, $\lim_{\upsilon \to -\infty} h(\upsilon) = +\infty$. Notice that $h'(\upsilon) = -1 - \tau k_3 e^{-\upsilon\tau} < 0$, then there is a negative constant λ for which $h(\lambda) = 0$ holds, i.e.,

$$\lambda - k_2 = k_3 e^{-\lambda\tau}. \tag{6}$$

For $t \in [-\tau, 0]$, it can be derived that

$$v(t) < k_1\overline{v}(0) \leq k_1\overline{v}(0)e^{\lambda t} + \frac{k_4}{-k_2-k_3}. \tag{7}$$

Then, we assert that

$$v(t) \leq k_1\overline{v}(0)e^{\lambda t} + \frac{k_4}{-k_2-k_3}, \tag{8}$$

where $t \in [0,T]$. In case this condition is not fulfilled, there exists a constant $t^* \in (0,T]$ that meets the inequalities:

$$v(t^*) > k_1\overline{v}(0)e^{\lambda t^*} + \frac{k_4}{-k_2-k_3}, \tag{9}$$

$$v(t) \leq k_1\overline{v}(0)e^{\lambda t} + \frac{k_4}{-k_2-k_3}, \ t \in [-\tau, t^*). \tag{10}$$

Based on (5) and (10), the computation can be made as:

$$\begin{aligned} v(t^*) \leq & k_1\overline{v}(0)e^{k_2 t^*} + \int_0^{t^*} e^{k_2(t^*-s)}[k_1 k_3\overline{v}(0)e^{\lambda(s-\tau)} \\ & + \frac{k_3 k_4}{-k_2-k_3} + k_4]\mathrm{d}s \end{aligned} \tag{11}$$

Using the above equation, and after calculating the definite integral with the help of (6), we deduce that

$$\begin{aligned} v(t^*) \leq & k_1\overline{v}(0)e^{k_2 t^*} + \frac{k_1 k_3\overline{v}(0)e^{k_2 t^* - \lambda\tau}}{\lambda - k_2}(e^{(\lambda-k_2)t^*} - 1) \\ & + \frac{k_4(1 - e^{k_2 t^*})}{-k_2-k_3} \\ \leq & k_1\overline{v}(0)e^{\lambda t^*} + \frac{k_4}{-k_2-k_3}. \end{aligned} \tag{12}$$

This result is in contradiction with (9), thereby corroborating the validity of our claim in (8). Therefore, for any $t \in [-\tau, T]$,

$$v(t) \leq k_1\overline{v}(0)e^{\lambda t} + \frac{k_4}{-k_2-k_3}. \tag{13}$$

(2) If $-k_3 e^{-k_2\tau} \leq k_2$, then define $v^*(t) = v(t)e^{-k_2 t}$. In terms of (5), we can infer that

$$\begin{aligned} v^*(t) \leq & k_1\overline{v}(0) + k_3\int_0^t e^{-k_2 s}v(s-\tau)\mathrm{d}s + k_4\int_0^t e^{-k_2 s}\mathrm{d}s \\ \leq & k_3 e^{-k_2\tau}\int_0^t v^*(s)\mathrm{d}s + k_4\int_0^t e^{-k_2 s}\mathrm{d}s \\ & + (k_1 + k_3\tau e^{-k_2\tau})\overline{v}(0). \end{aligned} \tag{14}$$

Subsequently, it can be inferred from the Gronwall-Bellman inequality that

$$v^*(t) \leq [(k_1 + k_3\tau e^{-k_2\tau})\overline{v}(0) + k_4 \int_0^t e^{-k_2 s}\mathrm{d}s]e^{k_3 e^{-k_2\tau}t},$$

that is,

$$v(t) \leq [(k_1+k_3\tau e^{-k_2\tau})\overline{v}(0)+k_4 \int_0^t e^{-k_2 s}\mathrm{d}s]e^{(k_3 e^{-k_2\tau}+k_2)t}.$$

This completes the proof. ■

Remark 1. *The delay integral inequalities in the existing literature were not sufficient to address the issues encountered in our research due to the intrinsic characteristics of time delays in the networks, which may bring essential changes to the dynamics of systems. Therefore, to facilitate our study, we introduced a new delay integral inequality by categorizing and examining different cases. From the inequality, we can deduce that if $-k_3e^{-k_2\tau} > k_2$, then $k_2 < 0$, leading to the conclusion that $k_2 < -k_3e^{-k_2\tau} < -k_3 < 0$. As a result, all possible cases for the coefficient k_2 in (5) are covered in Lemma 2. For a given time T, Lemma 2 indicates the FTB of system (5) under certain conditions. Moreover, if $k_2 = 0$, Lemma 2 reduces to the classical delay integral inequality, which has been considered in [31].*

Theorem 1. *Let (A_1) and (A_2) hold, then (1) is FTB concerning (T, κ_1, κ_2) over the class $\mathcal{F}(\eta)$ under either of the ensuing circumstances:*
(1) $z < -\zeta\frac{\prod_{i=1}^N \overline{\delta_i}^{2N_0}}{\prod_{j=1}^M \underline{\delta_j}^{2N_0}}$, $2N_0\sum_{i=1}^N \ln|\overline{\delta_i}| - 2N_0\sum_{j=1}^M \ln|\underline{\delta_j}| \leq \ln\kappa_2 - \ln\kappa_1$;
(2) $z \geq -\zeta\frac{\prod_{i=1}^N \overline{\delta_i}^{2N_0}}{\prod_{j=1}^M \underline{\delta_j}^{2N_0}}$, $2N_0\sum_{i=1}^N \ln|\overline{\delta_i}| - 2N_0\sum_{j=1}^M \ln|\underline{\delta_j}| + \ln(1+\zeta\tau e^{-z\tau}) + (\zeta\frac{\prod_{i=1}^N \overline{\delta_i}^{2N_0}}{\prod_{j=1}^M \underline{\delta_j}^{2N_0}}e^{-z\tau} + z)T \leq \ln\kappa_2 - \ln\kappa_1$,
where $z = 2\sum_{i=1}^N \frac{\ln|\overline{\delta_i}|}{T_{iA}} + 2\sum_{j=1}^M \frac{\ln|\underline{\delta_j}|}{T_{ja}} + 2 - 2\alpha\beta^2 - 2a_{\min} + \rho^2||\boldsymbol{B}||_F^2$, $\zeta = (||\boldsymbol{C}||_F^2 + 1)\rho^2$, $a_{\min} = \min\{a_1, a_2, \cdots, a_n\}$, and β is the Poincaré constant.

Proof: We introduce an auxiliary function $V(t) = ||\boldsymbol{u}(t,\boldsymbol{x})||^2$. For $t \in (t_{k-1}, t_k)$, the following expression is obtained:

$$\begin{aligned}\mathrm{d}V(t) =& 2(\boldsymbol{u}, \mathscr{A}\boldsymbol{u})\mathrm{d}t - 2(\boldsymbol{u}, \boldsymbol{A}\boldsymbol{u})\mathrm{d}t + 2(\boldsymbol{u}, \boldsymbol{B}\boldsymbol{f}(\boldsymbol{u}))\mathrm{d}t \\ &+ 2(\boldsymbol{u}, \boldsymbol{C}\boldsymbol{h}(\boldsymbol{u}(t-\tau,\boldsymbol{x})))\mathrm{d}t \\ &+ \mathrm{tr}(\boldsymbol{G}(\boldsymbol{u}(t-\tau,\boldsymbol{x}))Q\boldsymbol{G}^*(\boldsymbol{u}(t-\tau,\boldsymbol{x})))\mathrm{d}t \\ &+ 2(\boldsymbol{u}, \boldsymbol{G}(\boldsymbol{u}(t-\tau,\boldsymbol{x})))\mathrm{d}W(t,\boldsymbol{x}),\end{aligned} \tag{15}$$

which is obtained by the Itô formula as discussed in [40]. By integrating both sides of (15), one can obtain:

$$\begin{aligned}EV(t) =& EV(t_{k-1}) + \int_{t_{k-1}}^t E\Big[2(\boldsymbol{u}, \mathscr{A}\boldsymbol{u}) - 2(\boldsymbol{u}, \boldsymbol{A}\boldsymbol{u}) \\ &+ 2(\boldsymbol{u}, \boldsymbol{B}\boldsymbol{f}(\boldsymbol{u})) + 2(\boldsymbol{u}, \boldsymbol{C}\boldsymbol{h}(\boldsymbol{u}(s-\tau,\boldsymbol{x}))) \\ &+ ||\boldsymbol{G}(\boldsymbol{u}(s-\tau,\boldsymbol{x}))||_*^2\Big]\mathrm{d}s,\end{aligned} \tag{16}$$

which yields that

$$\begin{aligned}&D_-EV(t) \\ =&2E(\boldsymbol{u}, \mathscr{A}\boldsymbol{u}) - 2E(\boldsymbol{u}, \boldsymbol{A}\boldsymbol{u}) + 2E(\boldsymbol{u}, \boldsymbol{B}\boldsymbol{f}(\boldsymbol{u})) \\ &+ 2E(\boldsymbol{u}, \boldsymbol{C}\boldsymbol{h}(\boldsymbol{u}(t-\tau,\boldsymbol{x}))) + E||\boldsymbol{G}(\boldsymbol{u}(t-\tau,\boldsymbol{x}))||_*^2.\end{aligned} \tag{17}$$

Using the Poincaré Inequality, the Gauss formula and (A_1), we can infer that

$$E(\boldsymbol{u}, \mathscr{A}\boldsymbol{u}) \leq -\alpha E|||\boldsymbol{u}|||^2 \leq -\alpha\beta^2 EV(t), \tag{18}$$

Noting that $a_i > 0$, we have

$$-E(\boldsymbol{u}, \boldsymbol{A}\boldsymbol{u}) \leq -a_{\min}EV(t). \tag{19}$$

Integrating the Young inequality and (A_2) may lead to

$$\begin{aligned}2E(\boldsymbol{u}, \boldsymbol{B}\boldsymbol{f}(\boldsymbol{u})) \leq& EV(t) + \rho^2||\boldsymbol{B}||_F^2||\boldsymbol{u}||^2 \\ =&(\rho^2||\boldsymbol{B}||_F^2 + 1)EV(t).\end{aligned} \tag{20}$$

Similarly, we can ascertain that

$$\begin{aligned}&2E(\boldsymbol{u}, \boldsymbol{C}\boldsymbol{h}(\boldsymbol{u}(t-\tau,\boldsymbol{x}))) \\ \leq& EV(t) + \rho^2||\boldsymbol{C}||_F^2 EV(t-\tau),\end{aligned} \tag{21}$$

$$E||\boldsymbol{G}(\boldsymbol{u}(t-\tau,\boldsymbol{x}))||_*^2 \leq \rho^2 EV(t-\tau). \tag{22}$$

Hence, the expression can be deduced as follows:

$$\begin{aligned}D_-EV(t) \leq& (2 - 2\alpha\beta^2 - 2a_{\min} + \rho^2||\boldsymbol{B}||_F^2)EV(t) \\ &+ \zeta EV(t-\tau),\end{aligned} \tag{23}$$

where $t \in (t_{k-1}, t_k)$, and $\zeta = (||\boldsymbol{C}||_F^2 + 1)\rho^2$. At $t = t_k$, it holds that $EV(t_k^+) = \delta_k^2 EV(t_k)$. Then,

$$\begin{cases} D_-EV(t) \leq (2 - 2\alpha\beta^2 - 2a_{\min} + \rho^2||\boldsymbol{B}||_F^2)EV(t) \\ \qquad\qquad +\zeta EV(t-\tau),\ t \in (t_{k-1}, t_k), \\ EV(t_k^+) = \delta_k^2 EV(t_k), \\ EV(\theta) = E||\boldsymbol{\phi}(\theta, \boldsymbol{x}, \omega)||^2,\ \theta \in [-\tau, 0]. \end{cases}$$

For any given $\varepsilon > 0$, we assume that $v(t)$ satisfies the conditions defined by the following equations:

$$\begin{cases} D_-v(t) = (2 - 2\alpha\beta^2 - 2a_{\min} + \rho^2||\boldsymbol{B}||_F^2)v(t) \\ \qquad\qquad +\zeta v(t-\tau) + \varepsilon,\ t \in (t_{k-1}, t_k), \\ v(t_k^+) = \delta_k^2 v(t_k), \\ v(\theta) = E||\boldsymbol{\phi}(\theta, \boldsymbol{x}, \omega)||^2,\ \theta \in [-\tau, 0]. \end{cases}$$

In light of Lemma 1, it can be obtained that $EV(t) \leq v(t)$. The employment of the method of variation of parameters leads to the derivation that

$$v(t) = q(t,0)v(0) + \int_0^t q(t,s)(\zeta v(s-\tau) + \varepsilon)\mathrm{d}s, \tag{24}$$

where $q(t,s) = \exp((2 - 2\alpha\beta^2 - 2a_{\min} + \rho^2||\boldsymbol{B}||_F^2)(t-s))\prod_{t_i\in[s,t)}\delta_i^2$. Thus, from Definition 1, it can be deduced that

$$\begin{aligned}q(t,s) \leq& \exp\left((2 - 2\alpha\beta^2 - 2a_{\min} + \rho^2||\boldsymbol{B}||_F^2)(t-s)\right) \\ &\prod_{i=1}^N \overline{\delta_i}^{\frac{2(t-s)}{T_{iA}} + 2N_0} \prod_{j=1}^M \underline{\delta_j}^{\frac{2(t-s)}{T_{ja}} - 2N_0} \\ =& \frac{\prod_{i=1}^N \overline{\delta_i}^{2N_0}}{\prod_{j=1}^M \underline{\delta_j}^{2N_0}} e^{z(t-s)},\end{aligned}$$

where $z = 2\sum_{i=1}^{N}\frac{\ln|\overline{\delta_i}|}{T_{iA}} + 2\sum_{j=1}^{M}\frac{\ln|\underline{\delta_j}|}{T_{ja}} + 2 - 2\alpha\beta^2 - 2a_{\min} + \rho^2||\boldsymbol{B}||_F^2$, which implies that

$$\begin{aligned} & v(t) \\ \leq & \frac{\prod_{i=1}^{N}\overline{\delta_i}^{2N_0}}{\prod_{j=1}^{M}\underline{\delta_j}^{2N_0}}e^{zt}v(0) + \varepsilon\frac{\prod_{i=1}^{N}\overline{\delta_i}^{2N_0}}{\prod_{j=1}^{M}\underline{\delta_j}^{2N_0}}\int_0^t e^{z(t-s)}\mathrm{d}s \\ & + \zeta\frac{\prod_{i=1}^{N}\overline{\delta_i}^{2N_0}}{\prod_{j=1}^{M}\underline{\delta_j}^{2N_0}}\int_0^t e^{z(t-s)}v(s-\tau)\mathrm{d}s \\ \leq & \frac{\prod_{i=1}^{N}\overline{\delta_i}^{2N_0}}{\prod_{j=1}^{M}\underline{\delta_j}^{2N_0}}e^{zt}E||\boldsymbol{\phi}||_C^2 + \varepsilon\frac{\prod_{i=1}^{N}\overline{\delta_i}^{2N_0}}{\prod_{j=1}^{M}\underline{\delta_j}^{2N_0}}\int_0^t e^{z(t-s)}\mathrm{d}s \\ & + \zeta\frac{\prod_{i=1}^{N}\overline{\delta_i}^{2N_0}}{\prod_{j=1}^{M}\underline{\delta_j}^{2N_0}}\int_0^t e^{z(t-s)}v(s-\tau)\mathrm{d}s. \end{aligned} \tag{25}$$

Next, we will consider the following two cases.

Case 1: If $z < -\zeta\frac{\prod_{i=1}^{N}\overline{\delta_i}^{2N_0}}{\prod_{j=1}^{M}\underline{\delta_j}^{2N_0}} < 0$, then in accordance with Lemma 2, it can be derived that

$$v(t) \leq \frac{\prod_{i=1}^{N}\overline{\delta_i}^{2N_0}}{\prod_{j=1}^{M}\underline{\delta_j}^{2N_0}}E||\boldsymbol{\phi}||_C^2e^{\lambda t} + \frac{\varepsilon}{-z\frac{\prod_{j=1}^{M}\underline{\delta_j}^{2N_0}}{\prod_{i=1}^{N}\overline{\delta_i}^{2N_0}} - \zeta}, \tag{26}$$

where the constant $\lambda < 0$ meets the equation $\lambda - z = \zeta\frac{\prod_{i=1}^{N}\overline{\delta_i}^{2N_0}}{\prod_{j=1}^{M}\underline{\delta_j}^{2N_0}}e^{-\lambda\tau}$. Let $\varepsilon \to 0$, then we have $EV(t) \leq v(t) \leq \frac{\prod_{i=1}^{N}\overline{\delta_i}^{2N_0}}{\prod_{j=1}^{M}\underline{\delta_j}^{2N_0}}E||\boldsymbol{\phi}||_C^2e^{\lambda t}$. Therefore,

$$E||\boldsymbol{u}(t)||^2 \leq \frac{\prod_{i=1}^{N}\overline{\delta_i}^{2N_0}e^{\lambda t}E||\boldsymbol{\phi}||_C^2}{\prod_{j=1}^{M}\underline{\delta_j}^{2N_0}} \leq \frac{\kappa_1\prod_{i=1}^{N}\overline{\delta_i}^{2N_0}e^{\lambda t}}{\prod_{j=1}^{M}\underline{\delta_j}^{2N_0}} \leq \kappa_2.$$

Case 2: If $-\zeta\frac{\prod_{i=1}^{N}\overline{\delta_i}^{2N_0}}{\prod_{j=1}^{M}\underline{\delta_j}^{2N_0}} \leq z$, then we claim that the following inequality also holds:

$$-\zeta e^{-z\tau}\frac{\prod_{i=1}^{N}\overline{\delta_i}^{2N_0}}{\prod_{j=1}^{M}\underline{\delta_j}^{2N_0}} \leq z. \tag{27}$$

Indeed, for the case where $z \leq 0$, we have $e^{-z\tau} \geq 1$. Consequently, we can deduce that $-\zeta e^{-z\tau}\frac{\prod_{i=1}^{N}\overline{\delta_i}^{2N_0}}{\prod_{j=1}^{M}\underline{\delta_j}^{2N_0}} \leq -\zeta\frac{\prod_{i=1}^{N}\overline{\delta_i}^{2N_0}}{\prod_{j=1}^{M}\underline{\delta_j}^{2N_0}} \leq z$. On the other hand, when $z > 0$, it is evident that $-\zeta e^{-z\tau}\frac{\prod_{i=1}^{N}\overline{\delta_i}^{2N_0}}{\prod_{j=1}^{M}\underline{\delta_j}^{2N_0}} \leq 0 < z$.

Thus, applying Lemma 2, we have

$$\begin{aligned} & v(t) \\ \leq & \frac{\prod_{i=1}^{N}\overline{\delta_i}^{2N_0}}{\prod_{j=1}^{M}\underline{\delta_j}^{2N_0}}\big\{E||\boldsymbol{\phi}||_C^2\big(1+\zeta\tau e^{-z\tau}\big) + \\ & \varepsilon\int_0^t e^{-zs}\mathrm{d}s\big\}\exp\big\{\big(\zeta\frac{\prod_{i=1}^{N}\overline{\delta_i}^{2N_0}}{\prod_{j=1}^{M}\underline{\delta_j}^{2N_0}}e^{-z\tau} + z\big)t\big\}. \end{aligned} \tag{28}$$

Let $\varepsilon \to 0$, and $t \in [0, T]$, it then follows that

$$\begin{aligned} & E||\boldsymbol{u}(t)||^2 \\ \leq & \frac{\kappa_1\prod_{i=1}^{N}\overline{\delta_i}^{2N_0}}{\prod_{j=1}^{M}\underline{\delta_j}^{2N_0}}(1+\zeta\tau e^{-z\tau})\exp\big\{\big(\zeta\frac{\prod_{i=1}^{N}\overline{\delta_i}^{2N_0}}{\prod_{j=1}^{M}\underline{\delta_j}^{2N_0}}e^{-z\tau} + z\big)T\big\} \\ \leq & \kappa_2. \end{aligned}$$

This completes the proof. ■

Remark 2. *It can be inferred from Theorem 1 that the domain $\mathcal{O}$, the constant α, activation functions, impulses, and time delay τ may have an impact on the FTB of (1). More specifically, the Poincaré constant β in the criteria is influenced by the geometry of the domain $\mathcal{O}$, while the constant α depends on the reaction-diffusion matrix $\boldsymbol{D}(\boldsymbol{x})$. Additionally, the Lipschitz constant ρ is determined by the activation functions, and the impulsive strength δ_k and impulsive interval are affected by the impulses. It can also be deduced that, given $z \geq -\zeta\frac{\prod_{i=1}^{N}\overline{\delta_i}^{2N_0}}{\prod_{j=1}^{M}\underline{\delta_j}^{2N_0}}$, the time delays negatively affect the FTB of systems for $z \leq 0$, but positively influence it for $z > 0$.*

Remark 3. *Several studies on the FTB of impulsive systems have been conducted [17, 32–34]. In particular, in [32], the criteria of FTB on stabilizing impulses are established to be below a common threshold. Furthermore, [17] investigates the FTB of deterministic systems with stabilizing impulses and destabilizing impulses separately. However, systems with the stabilizing and destabilizing impulses concurrently, such as (1) have seldom been considered. We take these two kinds of impulses into account when modelling the neural networks, and avoid imposing the threshold on impulses, thereby extending some of the existing results. Theorem 1 further demonstrates that neural networks with hybrid impulses can robustly maintain their FTB, even in the presence of impulsive perturbations. Moreover, for networks where FTB is compromised due to such perturbations, restoration of FTB can be achievable through meticulous regulation of impulsive control strategies.*

Remark 4. *The parameter κ_2 serves as a predetermined threshold in our analysis, reflecting specific system requirements. Its value is not arbitrary, but instead, it is chosen based on the nature of the problem at hand and the system's intrinsic requirement. Within our current research context, the state is expected to remain below this threshold within a certain finite-time interval. While the selection of an optimal κ_2 value can indeed offer further insights into the system's behavior and possibly improve the method's performance, our study primarily focuses on validating the theoretical underpinnings of our proposed approach with a given κ_2. Future work might delve deeper into the optimization of κ_2 for various cases, ensuring the applicability and efficiency of the results in real-world scenarios.*

From the proof of Theorem 1, it is possible to establish the exponential stability of (1), although the concept of FTS differs from that of LAS.

Corollary 1. *Suppose that (A_1) and (A_2) hold, then (1) is exponentially stable in the mean-square sense over the class $\mathcal{F}(\eta)$ if $z < -\zeta\frac{\prod_{i=1}^{N}\overline{\delta_i}^{2N_0}}{\prod_{j=1}^{M}\underline{\delta_j}^{2N_0}}$, where $z = 2\sum_{i=1}^{N}\frac{\ln|\overline{\delta_i}|}{T_{iA}} + 2\sum_{j=1}^{M}\frac{\ln|\underline{\delta_j}|}{T_{ja}} + 2 - 2\alpha\beta^2 - 2a_{\min} + \rho^2||\boldsymbol{B}||_F^2$, and $\zeta = (||\boldsymbol{C}||_F^2 + 1)\rho^2$.*

Remark 5. *It is worth noting that Zhang et al. discussed the exponential stability of deterministic neural networks with impulses and time delays in [25]. When $\boldsymbol{D}(\boldsymbol{x}) = 0$ in (1),*

the conditions in our Corollary 1 align with those in [25], which implies that we extend some of their results. According to Theorem 1 and Corollary 1, if $z < -\zeta\frac{\prod_{i=1}^{N}\overline{\delta_i}^{2N_0}}{\prod_{j=1}^{M}\underline{\delta_j}^{2N_0}}$*, then (1) is exponentially stable, but not necessarily FTB. Furthermore, if Condition (2) in Theorem 1 is met, (1) will be FTB but not necessarily exponentially stable. Consequently, a system, which is exponentially stable may not satisfy the conditions of FTB, and vice versa, indicating that FTB and LAS are exactly distinct concepts. This can also be confirmed by Example 2(i) and Example 3(ii) in Section IV.*

In addition, the inequality (26) in the proof of Theorem 1 can also be used to derive the FTCB of (1).

Theorem 2. *Let* (A_1) *and* (A_2) *hold, then (1) is FTCB with respect to* $(T,\kappa_1,\kappa_2,\kappa_3,\sigma)$ *over the class* $\mathcal{F}(\eta)$*, if the first condition in Theorem 1 holds, and* $2N_0\sum_{i=1}^{N}\ln|\overline{\delta_i}| - 2N_0\sum_{j=1}^{M}\ln|\underline{\delta_j}| + \lambda(T-\sigma) \le \ln\kappa_3 - \ln\kappa_1$*, where* λ *is a negative constant such that* $\lambda = z + \zeta\frac{\prod_{i=1}^{N}\overline{\delta_i}^{2N_0}}{\prod_{j=1}^{M}\underline{\delta_j}^{2N_0}}e^{-\lambda\tau}$*,* $z = 2\sum_{i=1}^{N}\frac{\ln|\overline{\delta_i}|}{T_{iA}} + 2\sum_{j=1}^{M}\frac{\ln|\underline{\delta_j}|}{T_{ja}} + 2 - 2\alpha\beta^2 - 2a_{\min} + \rho^2||\boldsymbol{B}||_F^2$*, and* $\zeta = (||\boldsymbol{C}||_F^2 + 1)\rho^2$.

Particularly, when we let $\delta_k = 1$ in (1), the following results are obtained for the DRDSNNs without impulses.

Corollary 2. *When* (A_1) *and* (A_2) *are assumed to hold, (1) is FTB concerning* (T,κ_1,κ_2) *under either of the ensuing circumstances:*
(1) $z' < -\zeta$;
(2) $-\zeta \le z'$, $\ln(1+\zeta\tau e^{-z'\tau}) + (\zeta e^{-z'\tau} + z')T \le \ln\kappa_2 - \ln\kappa_1$,
where $z' = 2 - 2\alpha\beta^2 - 2a_{\min} + \rho^2||\boldsymbol{B}||_F^2$*, and* $\zeta = (||\boldsymbol{C}||_F^2 + 1)\rho^2$.
Moreover, (1) is FTCB with respect to $(T,\kappa_1,\kappa_2,\kappa_3,\sigma)$*, if the first condition in this corollary holds, and* $\lambda(T-\sigma) \le \ln\kappa_3 - \ln\kappa_1$*, where* $\lambda < 0$ *satisfies the equation* $\lambda = z' + \zeta e^{-\lambda\tau}$.

Remark 6. *Notice that the neural networks considered in Corollary 2 pertain to DRDSNNs without impulses, and the FTB has already been studied in [15]. Thus, the obtained results are more general, which would be further demonstrated by simulations of Example 2(ii) in Section IV.*

IV. Example

In this part of the paper, we provide a series of examples to validate the efficacy and practical applicability of the conclusions drawn from the above discussion.

Example 1. *We investigate the IDRDSNNs presented below.*

$$\begin{cases} \mathrm{d}u_1 = [0.95\triangle u_1 + 0.25(|u_1(t-0.1,x)+1| \\ \qquad -|u_1(t-0.1,x)-1|) - 0.3u_1 + 0.5u_2]\mathrm{d}t \\ \qquad +0.5\tanh(u_1(t-0.1,x))\mathrm{d}W,\ t \in (t_{k-1},t_k), \\ u_1(t_k^+) = p_k u_1(t_k),\ u_1(\theta) = 0.5\sin(0.5\pi x)\cos(1.4\theta), \\ \mathrm{d}u_2 = [0.95\triangle u_2 + 0.25(|u_1(t-0.1,x)+1| \\ \qquad -|u_1(t-0.1,x)-1|) - 0.3u_2 + 0.5u_1]\mathrm{d}t \\ \qquad +0.5\tanh(u_2(t-0.1,x))\mathrm{d}W,\ t \in (t_{k-1},t_k), \\ u_2(t_k^+) = p_k u_2(t_k),\ u_2(\theta) = 0.5\sin(0.5\pi x)\exp(\frac{\pi}{6}\theta), \\ u_1(t)|_{x\in\partial\mathcal{O}} = u_2(t)|_{x\in\partial\mathcal{O}} = 0,\ t \ge 0, \end{cases} \tag{29}$$

where $\theta \in [-0.1, 0]$, $x \in (-1, 1)$. *Take the impulsive sequence with* $\{t_k\} = \{0.4, 0.7, 0.8, 1.2, 1.4\}$, $p_1 = p_3 = p_4 = 0.8$, *and* $p_2 = p_5 = 1.3$, *then the average impulsive intervals are determined as* $T_{iA} = 0.7$, *and* $T_{ja} = 0.4$. *Let* $\beta = 1$, *and* $W = \sum_{n=1}^{\infty}\frac{1}{n}e_n(x)B_n(t)$, *with* $e_n(x) = \sqrt{0.5}\sin(0.5n\pi x)$, *and* $\{B_n(t)\}_{n=1}^{\infty}$ *representing a sequence of mutually independent standard Brownian motions. We specifically consider the case where* $\kappa_1 = 0.5$, $\kappa_2 = 7$, *and* $T = 2$. *This results in specific values for* $z = \frac{2\ln(1.3)}{0.7} + \frac{2\ln(0.8)}{0.4} - 2\times0.95 - 2\times0.3 + 0.5^2 + 2 = -0.6161 < 0$, $\zeta = 0.5$, *and* $2\ln(1.3) - 2\ln(0.8) + \ln(1 + 0.5\times0.1\times e^{-0.1z}) + (0.5\times\frac{1.3^2}{0.8^2}e^{-0.1z} + z)\times 2 = 2.5990 < \ln(7) - \ln(0.5) = 2.6391$. *These values satisfy the Condition (2) in Theorem 1. Based on the aforementioned parameters and initial conditions, we utilize Theorem 1 to demonstrate that (29) exhibits FTB regarding* $(2, 0.5, 7)$. *Then, we proceed by applying numerical discretization to (29) employing the method described in [41], which aids in deriving the solution to the neural network as specified in (29). The methodology for discretizing this differential equation is outlined below:*

$$\begin{cases} u_1^{i,k+1} = u_1^{i,k} + 0.95\frac{u_1^{i+1,k} - 2u_1^{i,k} + u_1^{i-1,k}}{(\triangle x)^2}\triangle t + 0.25\cdot \\ \qquad (|u_1^{i,k-0.1/\triangle t} + 1| - |u_1^{i,k-0.1/\triangle t} - 1|)\triangle t \\ \qquad -0.3u_1^{i,k}\triangle t + 0.5u_2^{i,k}\triangle t + 0.5\tanh(u_1^{i,k-0.1/\triangle t}) \\ \qquad \sum_{n=1}^{\infty}\frac{1}{n}e_n(i)[\sqrt{\triangle t}\xi_n + 0.5\triangle t(\xi_n^2 - 1)], \\ u_2^{i,k+1} = u_2^{i,k} + 0.95\frac{u_2^{i+1,k} - 2u_2^{i,k} + u_2^{i-1,k}}{(\triangle x)^2}\triangle t + 0.25\cdot \\ \qquad (|u_1^{i,k-0.1/\triangle t} + 1| - |u_1^{i,k-0.1/\triangle t} - 1|)\triangle t \\ \qquad -0.3u_2^{i,k}\triangle t + 0.5u_1^{i,k}\triangle t + 0.5\tanh(u_2^{i,k-0.1/\triangle t}) \\ \qquad \sum_{n=1}^{\infty}\frac{1}{n}e_n(i)[\sqrt{\triangle t}\xi_n + 0.5\triangle t(\xi_n^2 - 1)], \end{cases} \tag{30}$$

where $\triangle x = x^{i+1} - x^i$, $\triangle t = t^{k+1} - t^k$, *and* ξ_n *are the Gaussian random variables* $N(0,1)$. *Fig. 1 offers a visual representation of these findings, and depicts how the simulated behavior of (29) corroborates our theoretical results. Due to the stochastic perturbations, each simulation does not yield exactly the same results. To make the simulations more convincing, we conducted* 1000 *individual runs (the simulations presented in Fig. 3 and Fig. 4 are obtained in a similar manner). The state trajectories of* $||\boldsymbol{u}||^2$ *from these simulations are comprehensively presented, providing clear evidence for the FTB of (29), as illustrated in Fig. 2. It is worth noting that existing literature results cannot determine the FTB for (29), highlighting the significance of our novel approach. And it also demonstrates that the FTB of networks with impulsive control is maintained, even when subjected to impulsive perturbations.*

Example 2. *Taking the following DRDSNNs as an example*

$$\begin{cases} \mathrm{d}u = (0.2\triangle u + 0.75u)\mathrm{d}t + u(t-0.5,x))\mathrm{d}W, \\ \qquad t \in (t_{k-1},t_k) \\ u(t_k^+) = pu(t_k),\ t_k = 0.2k, k \in \mathbb{Z}_+, \\ u|_{x\in\partial\mathcal{O}} = 0,\ t \ge 0, \\ u(\theta) = \sin(0.5\pi x)\cos\theta, \end{cases} \tag{31}$$

where $\theta \in [-0.5, 0]$, $x \in (0, 20)$, *and* W *is the same as the one in Example 1 except* $e_n(x) = \sqrt{0.05}\sin(0.05n\pi x)$. *Take* $\beta = 0.05$, *and* $T = 2$.
(*i*) *For* $p = 0.5$, *our computations yield* $z = 2\ln(0.5)/0.2 +$

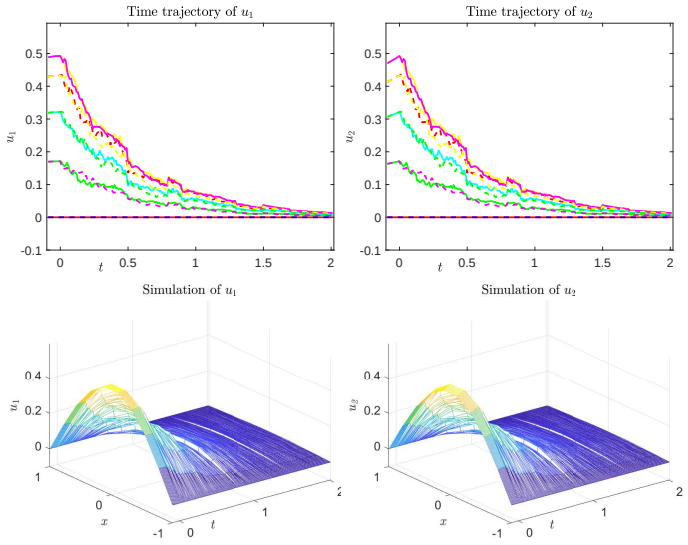

Fig. 1: State trajectories and simulations of u_1 and u_2 in Example 1.

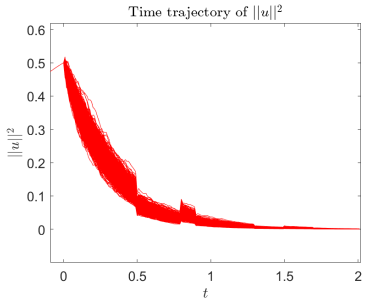

Fig. 2: State trajectory of $||\boldsymbol{u}||^2$ in Example 1.

$2 - 2 \times 0.2 \times 0.05^2 + 0.75^2 = -4.3700 < 0$, *and* $-\frac{\zeta}{p^2} = -4 > -4.3700$. *By applying Corollary 1, one can derive that (31) is exponentially stable. Refer to Fig. 3(a) where the convergence of the state is clearly depicted over time. However, a peculiar observation is that* $||u(0.19, x)||^2 = 13.1696$, *which exceeds* 12. *This indicates that (31) does not meet the FTB criteria for the parameter set* $(2, 10, 12)$. *But we have* $-2\ln(p_k) = 1.3863 < 1.4110 = \ln(41) - \ln(10)$, *which meet condition (1) in Theorem 1. One can also compute by MATLAB that* $\lambda = -0.1208$, *and* $-2\ln 0.5 - \lambda \times (2 - 0.5) = -1.5675 < \ln(3) - \ln(10) = -1.2040$. *Utilizing Theorem 1 and Theorem 2, following calculations leads us to a conclusion that both FTB for* $(2, 10, 41)$ *and FTCB for* $(2, 10, 41, 3, 0.5)$ *are achievable. These results are in line with the visual representation in Fig. 3(a), which showcases the systems's trajectory and convergence behavior.*

(ii) *When setting* $p = 1$, *then (31) transform into the reaction-diffusion stochastic neural networks without impulses, and we observe a different behavior. A visual examination of Fig. 3(b) reveals a non-converging state as time progresses. This diverging behavior signifies that the system no longer adheres to the FTB conditions for* $(2, 10, 41)$. *This also indicates that systems not initially exhibiting FTB (including those that become non-FTB due to impulsive disturbances) can achieve FTB by carefully designing impulsive control mechanisms.*

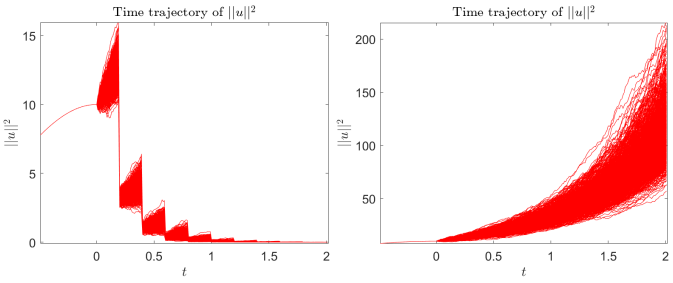

(a) (b)

Fig. 3: State trajectories of $||u||^2$ in Example 2

Example 3. *Examining the following DRDSNNs*

$$\begin{cases} \mathrm{d}u = (D\triangle u - u + 1.5u(t-\tau, x))\mathrm{d}t \\ \qquad +G\tanh u(t-\tau, x))\mathrm{d}W,\ t \in (t_{k-1}, t_k), \\ u(t_k^+) = pu(t_k),\ t_k = 0.32k,\ k \in \mathbb{Z}_+, \\ u|_{x\in\partial\mathcal{O}} = 0,\ t \geq 0, \\ u(\theta) = \sin(0.5\pi x)\cos\theta, \end{cases} \tag{32}$$

where $\theta \in [-\tau, 0]$, $x \in (0, 20)$, *and* W *is identical to the one in Example 2.*

(i) *Given* $D = 0.3$, $G = 1.5$, *and* $T = 2.3$. *For* $p = 1.16$, *we examine two distinct scenarios. With* $\tau = 5$, *we can calculate that* $z = 0.9261 > 0$, $\zeta = 4.5$ *and* $2\ln 1.16 + \ln(1 + 4.5 \times 5 \times e^{-0.9261\times 5}) + (4.5 \times 1.16^2 \times e^{-0.9261\times 5} + 0.9261) \times 2.3 = 2.7610 < \ln(160) - \ln(10) = 2.7726$. *These calculations suggest that (31) would be FTB with respect to* $(2.3, 10, 160)$. *Supporting this claim, the red trajectory in Fig. 4(a) does not exhibit significant divergence, and aligns with our theoretical predictions. On the other hand, when* $\tau = 0.1$, *the conditions for FTB concerning* $(2.3, 10, 160)$ *are not satisfied. This is visually evident in Fig. 4(a), where the black trajectory demonstrates a pronounced divergence, deviating significantly from a stable state. These findings indicate that for* $z > 0$, *time delays have a positive effect on the FTB of networks. Switching to* $p = 0.8$, *one can easily validate that the inequality* $-\zeta\frac{\prod_{i=1}^{N}\overline{\delta_i}^{2N_0}}{\prod_{j=1}^{M}\underline{\delta_j}^{2N_0}} < z < 0$ *is satisfied. Fig. 4(b) displays the time trajectory of* $||u||^2$ *for both* $\tau = 0.1$ *and* $\tau = 5$. *The graph clearly demonstrates the negative effect of time delays on the FTB of neural networks, particularly noticeable after being subjected to stabilizing impulses which result in* $z < 0$. *In conclusion, this examination provides a detailed insight into the FTB dynamics of neural networks subjected to different time delays and further strengthens the assertions made in Remark 2.*

(ii) *With* $D = 0.3$, $G = 1.5$, $\tau = 5$ *and* $T = 20$, *Fig. 4(c) presents the trajectories of* $||u(t)||^2$ *for different values of* p. *For* $p = 1.16$, *the trajectory is notably unstable, signifying that the system is not FTB with respect to* $(20, 10, 20)$. *For* $p = 1$ *and* $p = 0.5$, *both trajectories appear relatively steadier and less divergent, indicating that they meet the FTB conditions for* $(20, 10, 20)$. *However, it is interesting to note that the network with* $p = 1$ *does not exhibit the LAS behavior.*

(iii) *With parameters set at* $\tau = 5$, $p = 1.16$ *and* $T = 10$, *we explored the effects of the reaction-diffusion term and stochastic perturbations on the system's dynamics, as depicted in Fig. 4(d). Distinct dynamical characteristics emerge from*

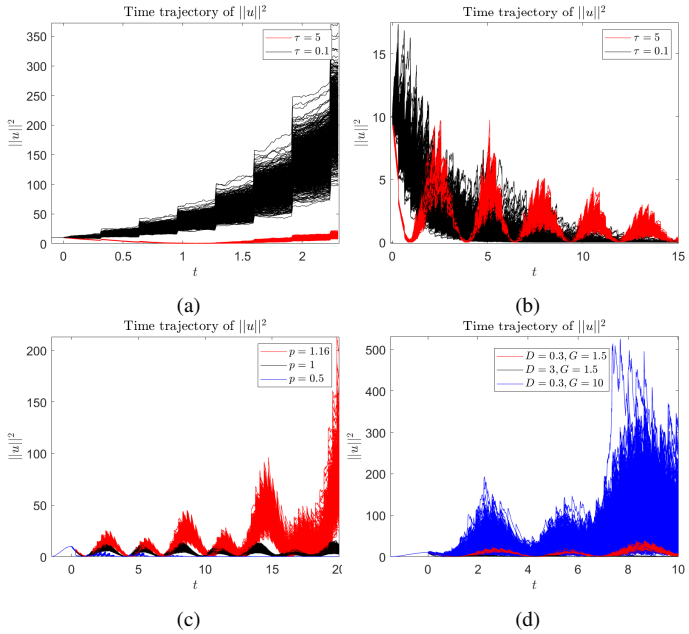

Fig. 4: State trajectories of $||u||^2$ in Example 3

the trajectories based on the chosen values of D and G. For $D = 0.3$ and $G = 1.5$, the red trajectory exhibits noticeable oscillations and fluctuations. Notably, the network maintains FTB concerning $(10, 10, 50)$. In contrast, with $D = 3$ and $G = 1.5$, the black trajectory stabilizes markedly quicker than its counterpart with $D = 0.3$ and $G = 1.5$. The behavior indicates the network is FTB with respect to both $(10, 10, 50)$ and $(10, 10, 15)$. However, when we set $D = 0.3$ and $G = 10$, the network deviates from the previously mentioned FTBs, and shows greater fluctuations. This pronounced oscillation suggests a compromised FTB for the neural networks due to the influence of stronger stochastic perturbations, represented by the increased value of G. In essence, these observations reveal the significant impact of the reaction-diffusion term and stochastic disturbances on the FTB of neural networks, which stresses the importance of considering such perturbations when analyzing the FTB.

Remark 7. *Example 2(i) implies that we cannot obtain the FTB of systems from LAS. Additionally, Example 3(ii) demonstrates that an FTB system may not necessarily be LAS. Consequently, FTB and LAS are independent concepts. Furthermore, Example 3 illustrates the impacts of delays, impulses, reaction-diffusion terms and stochastic perturbations on the FTB, respectively.*

Example 4. *We apply our theoretical results to image encryption to demonstrate their applicability. In order to generate signals for image encryption, we investigate the following neural network as the driving system:*

$$\begin{aligned} \mathrm{d}\boldsymbol{u} =& [\boldsymbol{D}\triangle\boldsymbol{u} - \boldsymbol{A}\boldsymbol{u} + \boldsymbol{B}\boldsymbol{f}(\boldsymbol{u}) + \boldsymbol{C}\boldsymbol{h}(\boldsymbol{u}(t-\tau,x))]\mathrm{d}t \\ &+ \boldsymbol{G}(\boldsymbol{u}(t-\tau,x))\mathrm{d}\boldsymbol{W}, \end{aligned} \tag{33}$$

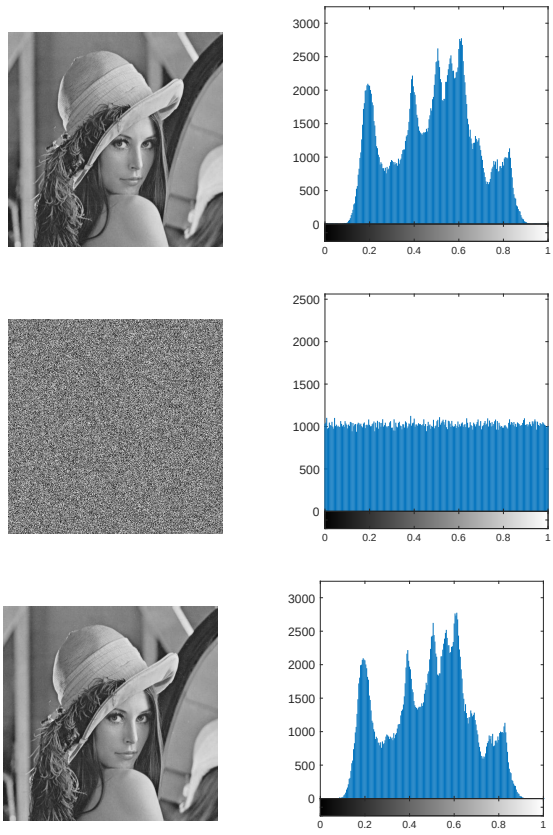

Fig. 5: The original, encrypted and decrypted Lena images (left) and corresponding histogram (right).

and the associated response system is as follows:

$$\begin{cases} \mathrm{d}\hat{\boldsymbol{u}} = [\boldsymbol{D}\triangle\hat{\boldsymbol{u}} - \boldsymbol{A}\hat{\boldsymbol{u}} + \boldsymbol{B}\boldsymbol{f}(\hat{\boldsymbol{u}}) + \boldsymbol{C}\boldsymbol{h}(\hat{\boldsymbol{u}}(t-\tau,x))]\mathrm{d}t \\ \qquad\quad +\boldsymbol{G}(\hat{\boldsymbol{u}}(t-\tau,x))\mathrm{d}\boldsymbol{W}, \ t \in (t_{k-1}, t_k), \\ \hat{\boldsymbol{u}}(t_k^+, x) = \delta_k\hat{\boldsymbol{u}}(t_k, x), \ k \in \mathbb{Z}_+, \end{cases} \tag{34}$$

where $x \in (0, 20)$, $\boldsymbol{D} = 10^{-4}\boldsymbol{I}$, $\boldsymbol{A} = \boldsymbol{I}$, $\boldsymbol{B} = \begin{pmatrix} 2 & -0.1 \\ -5 & 4.5 \end{pmatrix}$, $\boldsymbol{C} = \begin{pmatrix} -1.5 & -0.1 \\ -0.2 & -4 \end{pmatrix}$, $\boldsymbol{f}(\boldsymbol{u}) = \boldsymbol{h}(\boldsymbol{u}) = \tanh\boldsymbol{u}$, $\boldsymbol{G}(\boldsymbol{u}) = \begin{pmatrix} u_1 & 0 \\ 0 & u_2 \end{pmatrix}$, and $\boldsymbol{W}$ is the same as the one in Example 1. It follows from Theorem 1 and Theorem 2 that the error system is FTB and FTCB with certain parameters.

Then the results are applied to the image encryption algorithm proposed in [26]. Specifically, we first generate a chaotic decimal sequence as

$$S_{ij} = mod(round(||\boldsymbol{u}|| \times 10^8), 256). \tag{35}$$

where mod denotes the remained after the division operation. Then, each pixel of the original image is combined with the corresponding value in the S_{ij} matrix using an XOR operation to produce the encrypted image. The process for decryption is analogous to the encryption process, but the XOR operation is applied to each pixel of the encrypted image using the same S_{ij} matrix to retrieve the original image. To demonstrate the validity of the algorithm, we apply the encryption algorithm to two typical images: a gray image of

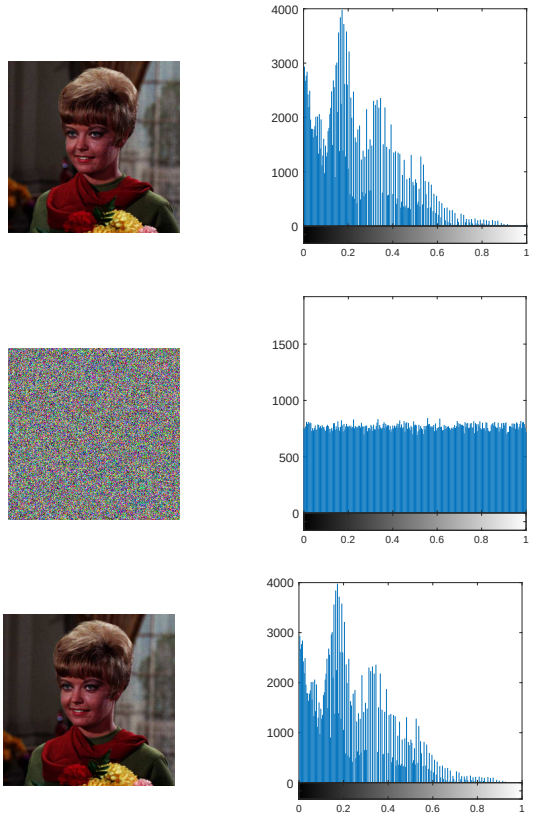

Fig. 6: The original, encrypted and decrypted Lady images (left) and corresponding histogram (right).

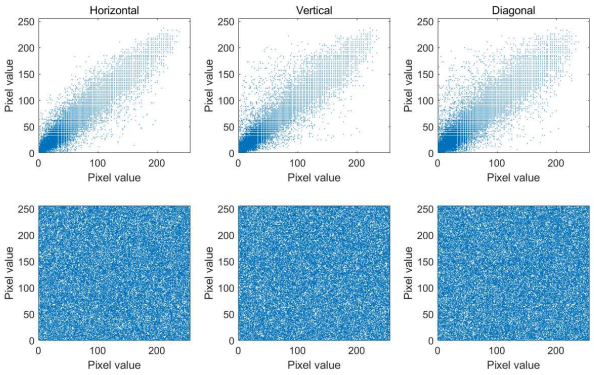

Fig. 7: The correlation map of adjacent pixels of original (top row) and encrypted (bottom row) Lady image from B channel in horizontal (left column), vertical (mid column) and diagonal (right column) directions.

Lena (512×512 *pixels) and a color image of Lady* (256×256 *pixels), both of which are commonly used for validating image encryption [26, 30, 42]. Fig. 5 and Fig. 6 display the original images, encrypted images and decrypted images of the two images, accompanied by their corresponding histograms. It is evident that the encrypted images and their histograms differ significantly from the original images, while the decrypted images closely resemble their respective original images. To further substantiate the effectiveness of the encryption, the correlation map of the adjacent pixels of Lady image (B channel) before and after encryption in horizontal, vertical and diagonal directions are presented in Fig. 7. This illustrates that the adjacent pixels shift from a high correlation to a minimal correlation upon encryption.*

Remark 8. *The example of image encryption given here is merely one instance of the numerous applications that can benefit from FTB. In fact, FTB has potential implications in various areas. For example, the application of FTB ensures that the position of the robotic arm remains stable within prescribed limits within a finite time, thereby enhancing both accuracy and reliability. Similarly, in the context of lane-keeping or collision-avoidance systems, FTB can set a strict timeframe within which the vehicle must return to a safe state, effectively reducing the risk of accidents.*

V. Conclusion

In this paper, a novel delay integral inequality has been established and used to derive sufficient criteria for the FTB and FTCB of IDRDSNNs. The effectiveness of our theoretical conclusions has been demonstrated through simulations of several numerical examples and applications in image encryption. It is worth noting that extending our results to systems with local Lipschitz conditions could yield more refined and nuanced insights. Such an extension might reflect real-world scenarios more accurately. We plan to delve into this in our subsequent studies, viewing it as a significant progression from our current work. Separately, we recognize that finite-time stability has been addressed in prior studies, which diverge from our current investigation and explore the asymptotic behavior of trajectories within a finite-time interval, as seen in [43–47]. Examining the finite-time stability for IDRDSNNs would indeed be a valuable direction for future research. Moreover, in the realm of neural networks, the importance of universal approximation capabilities is paramount. This aspect, involving rigorous theoretical analysis and simulations, will help us understand how IDRDSNNs can be effectively applied in a broader range of complex scenarios. Acknowledging this, our future work will also aim to investigate the universal approximation capabilities of IDRDSNNs, thereby expanding the scope of our research to encompass both the practical and theoretical dimensions of these networks.

References

[1] G. Kamenkov, "On stability of motion over a finite interval of time," *J. Appl. Math. Mech.*, vol. 17, no. 2, pp. 529–540, 1953.

[2] P. Dorato, "Short-time stability in linear time-varying systems," *Proc. IRE Int. Conv. Rec.,*, vol. Part 4, pp. 83–87, 1961.

[3] F. Amato, R. Ambrosino, M. Ariola, C. Cosentino, G. De Tommasi *et al.*, *Finite-time stability and control*. Springer, 2014, vol. 453.

[4] J. Song, Y. Niu, and Y. Zou, "Finite-time stabilization via sliding mode control," *IEEE Trans. Automat. Control*, vol. 62, no. 3, pp. 1478–1483, 2016.

[5] G. Garcia, S. Tarbouriech, and J. Bernussou, "Finite-time stabilization of linear time-varying continuous systems," *IEEE Trans. Automat. Control*, vol. 54, no. 2, pp. 364–369, 2009.

[6] F. Amato, G. De Tommasi, and A. Pironti, "Necessary and sufficient conditions for finite-time stability of impulsive dynamical linear systems," *Automatica*, vol. 49, no. 8, pp. 2546–2550, 2013.

[7] X. Li, X. Yang, and S. Song, "Lyapunov conditions for finite-time stability of time-varying time-delay systems," *Automatica*, vol. 103, pp. 135–140, 2019.

[8] F. Du and J.-G. Lu, "Finite-time stability of fractional-order fuzzy cellular neural networks with time delays," *Fuzzy Sets Syst.*, vol. 438, pp. 107–120, 2022.

[9] X. Yang and X. Li, "Finite-time stability of nonlinear impulsive systems with applications to neural networks," *IEEE Trans. Syst., Man, Cybern. Syst.*, 2021.

[10] L. Weiss and E. Infante, "Finite time stability under perturbing forces and on product spaces," *IEEE Trans. Automat. Control*, vol. 12, no. 1, pp. 54–59, 1967.

[11] J. Cheng, H. Xiang, H. Wang, Z. Liu, and L. Hou, "Finite-time stochastic contractive boundedness of markovian jump systems subject to input constraints," *ISA Trans.*, vol. 60, pp. 74–81, 2016.

[12] X. Zhang and C. Li, "Finite-time stability of nonlinear systems with state-dependent delayed impulses," *Nonlinear Dynam.*, vol. 102, no. 1, pp. 197–210, 2020.

[13] R. Rakkiyappan, G. Velmurugan, and J. Cao, "Finite-time stability analysis of fractional-order complex-valued memristor-based neural networks with time delays," *Nonlinear Dynam.*, vol. 78, no. 4, pp. 2823–2836, 2014.

[14] Z. Cai, L. Huang, M. Zhu, and D. Wang, "Finite-time stabilization control of memristor-based neural networks," *Nonlinear Anal. Hybrid Syst.*, vol. 20, pp. 37–54, 2016.

[15] M. S. Ali, S. Saravanan, and L. Palanisamy, "Stochastic finite-time stability of reaction-diffusion Cohen-Grossberg neural networks with time-varying delays," *Chinese journal of physics*, vol. 57, pp. 314–328, 2019.

[16] D. Efimov, A. Polyakov, E. Fridman, W. Perruquetti, and J.-P. Richard, "Comments on finite-time stability of time-delay systems," *Automatica*, vol. 50, no. 7, pp. 1944–1947, 2014.

[17] K.-N. Wu, M.-Y. Na, L. Wang, X. Ding, and B. Wu, "Finite-time stability of impulsive reaction-diffusion systems with and without time delay," *Appl. Math. Comput.*, vol. 363, p. 124591, 2019.

[18] R. Tang, X. Yang, P. Shi, Z. Xiang, and L. Qing, "Finite-time l_2 stabilization of uncertain delayed t-s fuzzy systems via intermittent control," *IEEE Trans. Fuzzy Syst.*, 2023.

[19] X. Li, X. Yang, and J. Cao, "Event-triggered impulsive control for nonlinear delay systems," *Automatica*, vol. 117, p. 108981, 2020.

[20] X. Liu, K. L. Teo, and B. Xu, "Exponential stability of impulsive high-order Hopfield-type neural networks with time-varying delays," *IEEE Trans. Neural Netw.*, vol. 16, no. 6, pp. 1329–1339, 2005.

[21] A. Jimenez-Triana, K. S. Tang, G. Chen, and A. Gauthier, "Chaos control in duffing system using impulsive parametric perturbations," *IEEE Trans. Circuits Syst. II. Express Briefs*, vol. 57, no. 4, pp. 305–309, 2010.

[22] S. Dong, X. Liu, S. Zhong, K. Shi, and H. Zhu, "Practical synchronization of neural networks with delayed impulses and external disturbance via hybrid control," *Neural Netw.*, vol. 157, pp. 54–64, 2023.

[23] S. Mohamad, K. Gopalsamy, and H. Akça, "Exponential stability of artificial neural networks with distributed delays and large impulses," *Nonlinear Anal. Real World Appl.*, vol. 9, no. 3, pp. 872–888, 2008.

[24] Z. Yang and D. Xu, "Stability analysis and design of impulsive control systems with time delay," *IEEE Trans. Automat. Control*, vol. 52, no. 8, pp. 1448–1454, 2007.

[25] W. Zhang, Y. Tang, J.-A. Fang, and X. Wu, "Stability of delayed neural networks with time-varying impulses," *Neural Netw.*, vol. 36, pp. 59–63, 2012.

[26] W.-H. Chen, S. Luo, and W. X. Zheng, "Impulsive synchronization of reaction-diffusion neural networks with mixed delays and its application to image encryption," *IEEE Trans. Neural Netw.*, vol. 27, no. 12, pp. 2696–2710, 2016.

[27] B. Ganesan, P. Mani, L. Shanmugam, and M. Annamalai, "Synchronization of stochastic neural networks using looped-lyapunov functional and its application to secure communication," *IEEE Trans. Neural Netw. Learn. Syst.*, 2022.

[28] Y. Sheng and Z. Zeng, "Impulsive synchronization of stochastic reaction-diffusion neural networks with mixed time delays," *Neural Netw.*, vol. 103, pp. 83–93, 2018.

[29] L. Hien, V. Phat, and H. Trinh, "New generalized Halanay inequalities with applications to stability of nonlinear non-autonomous time-delay systems," *Nonlinear Dyn.*, vol. 82, pp. 563–575, 2015.

[30] T. Wei, Q. Yao, P. Lin, and L. Wang, "Adaptive synchronization of stochastic complex dynamical networks and its application," *Neural Comput. Appl.*, vol. 31, pp. 6879–6892, 2019.

[31] J. K. Hale and S. M. V. Lunel, *Introduction to Functional Differential Equations*. Springer-Verlag, 1993.

[32] Y. Wang, X. Shi, Z. Zuo, M. Z. Chen, and Y. Shao, "On finite-time stability for nonlinear impulsive switched systems," *Nonlinear Anal. Real World Appl.*, vol. 14, no. 1, pp. 807–814, 2013.

[33] J. Tan and C. Li, "Finite-time stability of neural networks with impulse effects and time-varying delay," *Neural Process Lett.*, vol. 46, no. 1, pp. 29–39, 2017.

[34] R. Iervolino and R. Ambrosino, "Finite-time stabilization of state dependent impulsive dynamical linear systems," *Nonlinear Anal. Hybrid Syst.*, vol. 47, p. 101305, 2023.

[35] W. Liu and M. Röckner, *Stochastic Partial Differential Equations: An Introduction*. Springer, 2015.

[36] D. Xu and W. Zhou, "Existence-uniqueness and exponential estimate of pathwise solutions of retarded stochastic evolution systems with time smooth diffusion coefficients," *Discrete Contin. Dyn. Syst.*, vol. 37, no. 4, pp. 2161–2180, 2017.

[37] Q. Yao, L. Wang, and Y. Wang, "Periodic solutions to impulsive stochastic reaction-diffusion neural networks with delays," *Commun. Nonlinear Sci. Numer. Simul.*, vol. 78, p. 104865, 2019.

[38] J. Lu, D. W. Ho, and J. Cao, "A unified synchronization

criterion for impulsive dynamical networks," *Automatica*, vol. 46, no. 7, pp. 1215–1221, 2010.

[39] T. Wei, P. Lin, Y. Wang, and L. Wang, "Stability of stochastic impulsive reaction-diffusion neural networks with S-type distributed delays and its application to image encryption," *Neural Netw.*, vol. 116, pp. 35–45, 2019.

[40] L. Gawarecki and V. Mandrekar, *Stochastic Differential Equations in Infinite Dimensions: with Applications to Stochastic Partial Differential Equations*. Springer-Verlag Berlin Heidelberg, 2011.

[41] D. J. Higham, "An algorithmic introduction to numerical simulation of stochastic differential equations," *SIAM review*, vol. 43, no. 3, pp. 525–546, 2001.

[42] X. Song, J. Man, C. K. Ahn, and S. Song, "Synchronization in finite/fixed time for markovian complex-valued nonlinear interconnected neural networks with reaction-diffusion terms," *IEEE Trans. Neural Netw.*, vol. 8, no. 4, pp. 3313–3324, 2021.

[43] S. P. Bhat and D. S. Bernstein, "Continuous finite-time stabilization of the translational and rotational double integrators," *IEEE Trans. Automat. Control*, vol. 43, no. 5, pp. 678–682, 1998.

[44] J. Yin, S. Khoo, Z. Man, and X. Yu, "Finite-time stability and instability of stochastic nonlinear systems," *Automatica*, vol. 47, no. 12, pp. 2671–2677, 2011.

[45] D. Efimov and A. Aleksandrov, "On estimation of rates of convergence in Lyapunov-Razumikhin approach," *Automatica*, vol. 116, p. 108928, 2020.

[46] X. Li, D. W. Ho, and J. Cao, "Finite-time stability and settling-time estimation of nonlinear impulsive systems," *Automatica*, vol. 99, pp. 361–368, 2019.

[47] R. Tang, S. Yuan, X. Yang, P. Shi, and Z. Xiang, "Finite-time synchronization of intermittently controlled reaction-diffusion systems with delays: A weighted lkf method," *Commun. Nonlinear Sci. Numer. Simul.*, vol. 127, p. 107571, 2023.